Chapter 2
Robust Shared-Control for Rear-Wheel Drive Cars

Jingjing Jiang and Alessandro Astolfi

2.1 Introduction

Nowadays vehicles are one of the major means of transportation. The driving safety depends highly on the driver's attention, experience and skills. According to the report given by the World Health Organization, more than one million fatalities are caused by traffic-related accidents per year all over the world. To keep the human beings out of the vehicle control loop and to relieve them from the task of driving, researchers started to study self-driving cars.

A local path planning algorithm has been introduced in [12], in which the path modification is performed using a Voronoi cell when a collision is detected, while two path planning methods and multiple PID controllers have been used in [19] to achieve auto-driving. The paper [14] has presented a robust controller composed of a longitudinal controller and a lateral controller for a self-driving car to track a given trajectory. In [2] an electric race car is driven by a high-level navigation system via a multi-threaded program and an embedded low-level control to achieve accurate tracking of a straight line and good turning speed comparable to the human driver. Model Predictive Control (MPC) is also widely used in auto-driving cars. The paper [10] has used simulation and experimental results to demonstrate that smooth trajectory tracking with small position errors is achievable with the application of MPC. Other control methods, such as fuzzy control laws [13, 22], adaptive controls [15, 17], and sliding mode controls [4], have also been utilized in vehicle auto-navigation.

J. Jiang (✉) · A. Astolfi
Dept. of Electrical and Electronic Engineering, Imperial College London,
London SW7 2AZ, UK
e-mail: jingjing.jiang10@imperial.ac.uk

A. Astolfi
The DICII, University of Roma "Tor Vergata", Via Del Politecnico 1, 00133 Rome, Italy
e-mail: a.astolfi@imperial.ac.uk

Y. Wang and F. Zhang (eds.), *Trends in Control and Decision-Making for Human–Robot Collaboration Systems*, DOI 10.1007/978-3-319-40533-9_2

Even though the driverless cars, such as Google Cars, have already been successfully tested in some areas, they still have several limitations. For instance, much intricate preparations have to be made before Google Cars can be driven on a certain road. Data have to be studied carefully after the testing drive, meter by meter, by both computers and humans. Even though the sensors of the car can detect obstacles on the road, they may be unable to distinguish between a rock and a crumpled piece of paper. Therefore the car will drive around both of them. Compared with auto driving, the cooperative driving which does not abandon the human driver has several advantages: it provides additional information (beyond those sensed directly by vehicle-based sensors) and better quality of information (lower noise and smaller delays), and is able to enable direct negotiations about maneuvers (such as merging and creating gaps) [20]. A shared-control algorithm for a car has been proposed in [11] and [5]: the car is able to drive autonomously by following the path created by waypoints generated by the human operator, while a passive human–machine interface has been utilized in [16] to suggest control actions to the driver of a vehicle with n-trailers. A longitudinal driving-assistance system based on a self-learning algorithm for the driver modeling and an automatic braking activation (or collision warning) system has been studied in [21]. A human-in-the-loop design approach to the control of a smart car based on a supervisory control that determines the desired velocity for the vehicle has been presented in [1]. Differently from the traditional braking model, the paper [3] has proposed a new safety indicator, named as "time gap interval", for the safe distance to the car in front in car-following situations. The paper [8] has presented a shared-control algorithm for the kinematic model of a rear-wheel drive car to "correct" the driver's behaviors in "dangerous" situations. The design is based on the measurement of absolute positions. This chapter studies the human–robot cooperation, extends the results given in [8] to the cases in which no absolute positions are available and to the cases in which disturbances are taken into consideration, thus also extending [9]. The shared controller established in the chapter is designed to assist the human driver drive safely.

The rest of the chapter is organized as follows. In Sect. 2.2 the shared-control problem for the kinematic model of a rear-wheel drive car is formulated. The solutions to the problem with and without measurements of absolute positions are given in Sects. 2.3 and 2.5, respectively. Formal properties of the closed-loop system with shared control are presented in each section. To deal with model uncertainties, we consider the system with the presence of bounded disturbances as explained in Sect. 2.4. Three case studies showing the effectiveness of the shared-control algorithm are provided in Sect. 2.6. Finally, some conclusions and suggestions for future work are given in Sect. 2.7.

2.2 Problem Formulation, Definitions, and Assumptions

The chapter studies the kinematic model of a rear-wheel drive car, the dynamics of which, as explained in [8], are described by the equations

$$\begin{aligned} \dot{x} &= v_s \cos\theta, \\ \dot{y} &= v_s \sin\theta, \\ \dot{\theta} &= \frac{v_s \tan\phi}{l}, \\ \dot{\phi} &= \omega_s, \end{aligned} \tag{2.1}$$

where (x, y) are the coordinates of the middle point of the rear-axle, θ and ϕ are the inertial heading and the steering angle, respectively. l denotes the distance between the front-axle and the rear-axle. Furthermore, the shared-control inputs are the forward velocity v_s and the angular velocity of front wheels ω_s.

As explained in Sect. 2.1 the shared-control input $u_s = [v_s, \omega_s]^T$ discussed in this chapter is a combination of the human input $u_h = [v_h, \omega_h]^T$, named as *h-control*, and the feedback control input $u_f = [v_f, \omega_f]^T$, named as *f-control*. Figure 2.1 illustrates the architecture of the system with the shared controller, where "H" describes the human action. Define u_s as

$$u_s(t) = (1 - k(t))u_f(t) + k(t)u_h(t), \tag{2.2}$$

where $k(t) \in [0, 1]$ is named as *sharing function*, describing how the control authority is shared between the driver and the feedback controller. The value of k can provide feedback to the driver indicating how safe his/her behavior is. This is helpful to improve the driver's performance, especially for new drivers. Figure 2.1 also shows that the human driver receives more information than the feedback controller since he/she is able to directly perceive the environment besides reading data from the sensors.

In this chapter, we use the subscripts h, f, and s to denote the control inputs generated by the human operator, the feedback controller, and the shared controller, respectively.

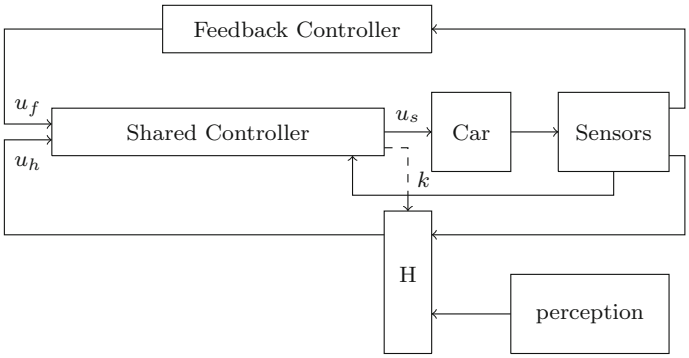

Fig. 2.1 The proposed architecture of the shared-control

Definition 2.1 Similar to [8], the names *s-closed-loop* and *h-closed-loop* are used to represent the closed-loop system with shared control u_s (described by (2.1)) and human control u_h, respectively.

Let $\mathcal{P}_a(t) \in \mathbb{R}^2$ be a compact set describing the admissible Cartesian configuration set[1] of the system (2.1) and u_h be a given h-control. Then the shared-control problem for the kinematic model of the car can be formulated as follows.

Given the system (2.1), a compact nonempty set $\mathcal{P}_a(t)$ and an h-control $u_h(t)$, find (if possible)

- an f-control u_f;
- a sharing function k;
- a safe set $\mathcal{R}_s(v_h, t) \triangleq \mathcal{P}_a(t) \times \mathcal{H}_s \times \mathcal{A}_s \subset \mathcal{P}_a(t) \times \mathcal{H} \times \mathcal{A} \triangleq \mathcal{R}(v_h, t)$;

where $\mathcal{H}$ and $\mathcal{A}$ are the sets of heading angles and steering angles, respectively, such that the s-closed-loop system (2.1) and (2.2) has the following properties.

(1) The (x, y)-position of the car remains in its feasible Cartesian configuration set, *i.e.,* $(x(t), y(t)) \in \mathcal{P}_a(t)$ for all $t \geq 0$.
(2) The shared controller does not change the aims of the human driver if he/she drivers safely, *i.e.,*

$$\Omega_s = \begin{cases} \Omega_h & \text{if } \Omega_h \subset \mathcal{R}_s(v_h, t), \\ \Pi_{\mathcal{R}_s}(\Omega_h) & \text{if } \Omega_h \not\subset \mathcal{R}_s(v_h, t), \end{cases}$$

where Ω_s and Ω_h are the Ω-limit sets of the s-closed-loop system and h-closed-loop system, respectively. $\Pi_{\mathcal{R}_s}(\Omega_h)$ is the projection of Ω_h into the safe subset $\mathcal{R}_s(v_h, t)$, which will be defined in Sects. 2.3.1 and 2.5.1, with and without measurements of absolute positions, respectively.
(3) $u_s(t) = u_h(t)$ for all $t \geq 0$ such that the system state belongs to $\mathcal{R}_s(v_h, t)$.

Note that for any fixed v_h, $\mathcal{H}_s$ and $\mathcal{A}_s$ denote the sets of all heading angles and steering angles such that the car is unable to hit the boundary of $\mathcal{P}_a$ within an arbitrary short period of time, respectively.

Assumption 2.1 We assume that the projection of the car in the (x, y)-plane is a rectangle with length l and width w, where l denotes the distance between the middle of the front-axle and the middle of the rear-axle and w denotes the distances between the centers of the two rear wheels (or the centers of the two front wheels).

[1] We use $(x(t), y(t))$ to denote the Cartesian coordinates of the center of the rear-axle at the time instant t. The admissible Cartesian configuration set $\mathcal{P}_a(t)$ is such that

$$(x(t), y(t)) \in \mathcal{P}_a(t), \text{ for all } t \geq 0.$$

.

2.3 Design of the Shared-Control Law with Measurements of Absolute Positions

In this section, we provide a shared-control algorithm for the kinematic model of a rear-wheel drive car with measurements of absolute positions.

Assumption 2.2 We assume that the admissible Cartesian configuration set $\mathcal{P}_a$ is defined by a group of linear inequalities given by

$$\mathcal{P}_a = \{p \in \mathbb{R}^2 \,|Sp + T \leq 0\}, \tag{2.3}$$

where $p = [x, y]^T$, $S = [s_1^T, s_2^T, \ldots, s_m^T]^T \in \mathbb{R}^{m\times 2}$ and $T = [t_1, t_2, \ldots, t_m]^T \in \mathbb{R}^m$. In addition, if $m > 2$, the matrices S and T are such that

$$\text{rank}(\begin{bmatrix} s_{r_1} \\ \vdots \\ s_{r_g} \end{bmatrix}) < \text{rank}(\begin{bmatrix} s_{r_1} & t_{r_1} \\ \vdots & \vdots \\ s_{r_g} & t_{r_g} \end{bmatrix}),$$

for all $g \in [3, m]$ and $r_1, r_2, \ldots, r_g \in \{1, 2, \ldots, m\}$.

2.3.1 Design of the Feedback Controller

Lemma 2.1 *Consider the set $\mathcal{P}_a$ in (2.3) and assume Assumption 2.2 holds. Then for any fixed v_h and θ no more than two constraints are active[2] at any given time instant.*

Proof If $m \leq 2$ then the claim trivially holds. Consider now the case $m \geq 3$. We prove the claim by contradiction. Suppose that at a given time instant, for a fixed v_h and θ, three constraints are active. Without loss of generality assume that these are the first 3 constraints. Then there exists a positive constant η such that

$$\begin{bmatrix} s_1 \\ s_2 \\ s_3 \end{bmatrix} \left(p + \eta \begin{bmatrix} v_h \cos\theta \\ v_h \sin\theta \end{bmatrix} \right) + \begin{bmatrix} t_1 \\ t_2 \\ t_3 \end{bmatrix} = 0.$$

By Assumption 2.2 the above equation does not have any solutions, hence the claim.

As detailed in [6] the m inequality constraints can be partitioned into N_c groups, where $N_c \leq \binom{m}{2}$. Each group contains two constraints. Relative to the i^{th} group of

[2]For each human input v_h and heading angle θ, the i^{th} constraint is active at position p if there exists a positive η such that $s_i \left(p + \eta \begin{bmatrix} v_h \cos\theta \\ v_h \sin\theta \end{bmatrix} \right) + t_i = 0$. As a results, the constraint is said to be "active" if the car is moving towards the constraint.

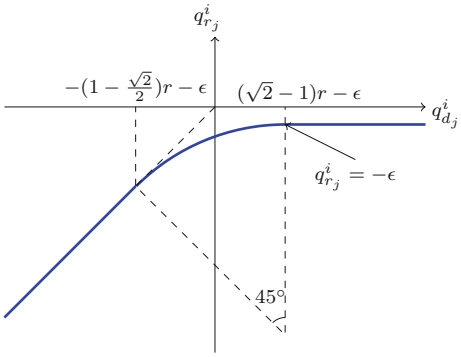

Fig. 2.2 Graph of the function $q^i_{r_j}$ given by (2.6) for $j \in \{1, 2\}$

constraints, *i.e.*,

$$q^i = S^i p + T^i \leq 0, \tag{2.4}$$

where S^i is invertible, we define a new variable $z^i = [z^i_1, z^i_2]^T$, with

$$z^i_j = \log \frac{q^i_j}{q^i_{r_j}}, \tag{2.5}$$

for all $j \in \{1, 2\}$, where $q^i_{r_j}$ is the reference signal relative to q^i_j and is defined by

$$q^i_{r_j} = \begin{cases} q^i_{d_j}, & \text{if } q^i_{d_j} \leq (1-\frac{\sqrt{2}}{2})r-\epsilon, \\ -\epsilon, & \text{if } q^i_{d_j} \geq (\sqrt{2}-1)r-\epsilon, \\ -(r+\epsilon)+\sqrt{r^2-[(\sqrt{2}-1)r-\epsilon-q^i_{d_j}]^2}, & \text{otherwise}, \end{cases} \tag{2.6}$$

where r is a user-selected positive constant, ϵ is a sufficiently small positive number, $q^i_d = [q^i_{d_1}, q^i_{d_2}]^T = S^i p_d + T^i$ and p_d describes the desired trajectory in the space $\mathcal{P}$. Note that the definition of $q^i_{r_j}$ is illustrated in Fig. 2.2 and $[S^{i\,-1}(q^i_r - T^i)]$ is the projection of p_d into the admissible Cartesian configuration set $\mathcal{P}_a$ relative to the i^{th} group of constraints.

It is clear that $q^i_{r_j}$ is a smooth function taking negative values. Therefore, $\dot{q}^i_{r_j}$ exists. Let $\alpha^i_r = [\alpha^i_{r_1}, \alpha^i_{r_2}]^T = S^{i\,-1}\dot{q}^i_r$. Then[3]

[3]The definition of the function atg(·), given in [8], is close to that of the standard four quadrant arctan function except that its range equals to $(-\infty, +\infty)$ rather than $[-\pi, \pi)$. In addition, it is a smooth function with values in the range $(-\infty, +\infty)$. Therefore $\dot{\theta}^i_r$ always exist, which is a necessary condition for calculating $\dot{L}^i$, where L^i is given by (2.9).

$$\begin{aligned} p_r^i &= S^{i^{-1}}(q_r^i - T^i),\ \theta_r^i = \text{atg}(\alpha_{r_2}^i, \alpha_{r_1}^i), \\ v_r^i &= \sqrt{{\alpha_{r_1}^i}^2 + {\alpha_{r_2}^i}^2},\quad \phi_r^i = \text{atan}\left(\frac{\dot{\theta}_r^i l}{v_r^i}\right), \\ \omega_r^i &= \dot{\phi}_r^i. \end{aligned} \tag{2.7}$$

Let $(p_d, \theta_d, \phi_d) \in \Omega_h$, then the projection of (p_d, θ_d, ϕ_d) into the safe subset $\mathcal{R}_s^i$ is defined as

$$\Pi_{\mathcal{R}_s}^i(p_d, \theta_d, \phi_d) = (p_r^i, \theta_r^i, \phi_r^i),$$

where $(p_r^i, \theta_r^i, \phi_r^i)$ is given by (2.7). Furthermore, the projection of Ω_h into the set $\mathcal{R}_s^i$ is defined as

$$\Pi_{\mathcal{R}_s}^i(\Omega_h) = \{s \in \mathcal{R}_s | s = \Pi_{\mathcal{R}_s}^i(p_d, \theta_d, \phi_d)\}, \quad \forall (p_d, \theta_d, \phi_d) \in \Omega_h.$$

System (2.1) controlled by the feedback controller u_f^i can be rewritten, using the variable z^i, as

$$\begin{aligned} \dot{z}_1^i &= \frac{v_f^i \cos\theta^i}{e^{z_1^i} q_{r_1}^i} - \frac{v_r^i \cos\theta_r^i}{q_{r_1}^i}, \\ \dot{z}_2^i &= \frac{v_f^i \cos\theta^i}{e^{z_2^i} q_{r_2}^i} - \frac{v_r^i \cos\theta_r^i}{q_{r_2}^i}, \\ \dot{\theta}^i &= \frac{v_f^i \tan\phi^i}{l}, \\ \dot{\phi}^i &= \omega_f^i. \end{aligned} \tag{2.8}$$

Let

$$\theta^{i*} = \text{atg}(e^{z_2^i}(v_r^i \sin\theta_r^i - \gamma_2 z_2^i), e^{z_1^i}(v_r^i \cos\theta_r^i - \gamma_1 z_1^i)),$$

$$\phi^{i*} = \text{atg}\left(\begin{array}{c} l\dfrac{z_1^i}{e^{z_1^i} q_{r_1}^i} \sin\dfrac{\theta + \theta^{i*}}{2} \text{sinc}\dfrac{\theta - \theta^{i*}}{2} + \dfrac{\theta^{i*} l}{v_f^i} \\ -l\dfrac{z_2^i}{e^{z_2^i} q_{r_2}^i} \cos\dfrac{\theta + \theta^{i*}}{2} \text{sinc}\dfrac{\theta - \theta^{i*}}{2} \end{array}, 1 \right),$$

where $\gamma_1 > 0$, $\gamma_2 > 0$.

Consider the Lyapunov function candidate relative to the i^{th} group of constraints (2.4) given by

$$L^i(z_1^i, z_2^i, \theta^i, \phi^i) = \frac{1}{2}[{z_1^i}^2 + {z_2^i}^2 + (\theta^i - \theta^{i*})^2 + (\tan\phi^i - \tan\phi^{i*})^2], \tag{2.9}$$

and choose $u_f^i = [v_f^i, \omega_f^i]^T$ such that $L^i < 0$ for all $(z_1^i, z_2^i, \theta^i, \phi^i) \neq (0, 0, \theta^{i*}, \phi^{i*})$. One such choice is given by

$$v_f^i = \sqrt{e^{2z_1^i}(v_r^i \cos\theta_r^i - \gamma_1 z_1^i)^2 + e^{2z_2^i}(v_r^i \sin\theta_r^i - \gamma_2 z_2^i)^2},$$
$$\omega_f^i = \cos^2\phi^i \left[-\frac{v(\theta^i - \theta^{i*})}{l} + \frac{\dot{\phi}^{i*}}{\cos^2\phi^{i*}} - \gamma_3(\tan\phi - \tan\phi^{i*}) \right],$$

which yields

$$\dot{L}^i = \gamma_1 \frac{{z_1^i}^2}{q_{r_1}^i} + \gamma_2 \frac{{z_2^i}^2}{q_{r_2}^i} - \gamma_3(\tan\phi - \tan\phi^*)^2 \leq 0.$$

This can be "pulled back" into the (p, θ, ϕ) coordinates by

$$v_f^i = \sqrt{\left(\frac{q_1^i}{q_{r_1}^i}\right)^2 \left(v_r^i \cos\theta_r^i - \gamma_1 \log\frac{q_1^i}{q_{r_1}^i}\right)^2 + \left(\frac{q_2^i}{q_{r_2}^i}\right)^2 \left(v_r^i \sin\theta_r^i - \gamma_2 \log\frac{q_2^i}{q_{r_2}^i}\right)^2},$$
$$\omega_f^i = \cos^2\phi^i \left[-\frac{v(\theta^i - \theta^{i*})}{l} + \frac{\dot{\phi}^{i*}}{\cos^2\phi^{i*}} - \gamma_3(\tan\phi - \tan\phi^{i*}) \right], \tag{2.10}$$

where

$$\phi^{i*} = \mathrm{atg}\left(\begin{array}{c} l\dfrac{\log\frac{q_1^i}{q_{r_1}^i}}{q_1^i} \sin\dfrac{\theta + \theta^{i*}}{2} \mathrm{sinc}\dfrac{\theta - \theta^{i*}}{2} + \dfrac{\theta^{i*} l}{v_f^i} \\ -l\dfrac{\log\frac{q_2^i}{q_{r_2}^i}}{q_2^i} \cos\dfrac{\theta + \theta^{i*}}{2} \mathrm{sinc}\dfrac{\theta - \theta^{i*}}{2} \end{array} , 1 \right),$$
$$\theta^{i*} = \mathrm{atg}\left(\frac{q_2^i}{q_{r_2}^i} \left(v_r^i \cos\theta_r^i - \gamma_2 \log\frac{q_2^i}{q_{r_2}^i} \right), \frac{q_1^i}{q_{r_1}^i} \left(v_r^i \cos\theta_r^i - \gamma_1 \log\frac{q_1^i}{q_{r_1}^i} \right) \right), \tag{2.11}$$

and $q_j^i = s_j^i p + t_j^i$, $q_{r_j}^i = s_j^i p_r + t_j^i$ for all $j \in \{1, 2\}$.

2.3.2 *Shared-Control Algorithm*

The overall set $\mathcal{R}$, denoting the set of all feasible values of the system states, can be partitioned into three subsets: the safe subset $\mathcal{R}_s$, the hysteresis subset $\mathcal{R}_h$ and the dangerous subset $\mathcal{R}_d$. The set division is based on the distance between the current (x, y)-position and the boundary of the set $\mathcal{P}_a$ and the velocity towards the boundary. Relative to the i^{th} group of constraints, the three subsets are defined by (12) given on the top of next page,

$$\tilde{\mathcal{R}}_s^i(v_h) = \left\{ (q^i, \theta^i, \phi^i) \in \mathcal{Q}_a^i \times \mathcal{H} \times \mathcal{A} : m_j^i < \frac{1}{q_j^i + b_2} - \frac{1}{b_2} \text{ if } q_j^i \geq -b_2 \text{ for all } j \in \{1, 2\} \right\}$$

$$\tilde{\mathcal{R}}_h^i(v_h) = \left\{ \begin{array}{l} (q^i, \theta^i, \phi^i) \in \mathcal{Q}_a^i \times \mathcal{H} \times \mathcal{A} : \quad m_j^i \leq \dfrac{1}{q_j^i + b_1} - \dfrac{1}{b_1} \text{ if } q_j^i \geq -b_1 \\ \qquad\qquad \text{for all } j \in \{1, 2\} \\ \qquad\qquad \text{and } \exists k \in \{1, 2\} \text{ such that} \\ \qquad\qquad m_k^i \geq \dfrac{1}{q_k^i + b_2} - \dfrac{1}{b_2} \text{ and } q_k^i \geq -b_2 \end{array} \right\} \tag{12}$$

$$\tilde{\mathcal{R}}_d^i(v_h) = \left\{ \begin{array}{l} (q^i, \theta^i, \phi^i) \in \mathcal{Q}_a^i \times \mathcal{H} \times \mathcal{A} : \qquad \exists j \in \{1, 2\} \text{ such that} \\ \qquad\qquad m_j^i > \dfrac{1}{q_j^i + b_1} - \dfrac{1}{b_1}, -b_1 \leq q_j^i < 0 \\ \qquad\qquad \text{or } \exists j \in \{1, 2\} \text{ such that} \\ \qquad\qquad m_j^i > \dfrac{1}{q_j^i + b_1} - \dfrac{1}{b_1}, q_j^i = 0 \end{array} \right\}$$

where[4] $\mathcal{Q}_a^i = S^i \mathcal{P}_a + T^i$, $b_2 > b_1 > 0$, $m_j^i = s_j^i [\cos\theta^i, \sin\theta^i]^T v_h$ and $m_k^i = s_k^i [\cos\theta^i, \sin\theta^i]^T v_h$ with $k, j \in \{1, 2\}$.

Example 2.1 Assume that the admissible Cartesian configuration set $\mathcal{P}_a$ is a square described by (2.3), where $S = [a_1^T, a_2^T, a_3^T, a_4^T]^T$ and $T = [-3, -3, -3, -3]^T$ with $a_1 = [-1, 0]$, $a_2 = [1, 0]$, $a_3 = [0, -1]$ and $a_4 = [0, 1]$. Figure 2.3 on the top of next page provides graphical illustrations of the three subsets for different values of v_h and θ.

Note that this definition is given in the (q^i, θ^i, ϕ^i) coordinates and can be transferred to the (x, y, θ^i, ϕ^i) coordinates by the equations

$$\begin{aligned} \mathcal{R}_s^i(v_h) &= \mathrm{diag}(\mathrm{S}^{\mathrm{i}-1}, \mathrm{I})(\tilde{\mathcal{R}}_{\mathrm{s}}^{\mathrm{i}} - \mathrm{col}(\mathrm{T}^{\mathrm{i}}, 0)), \\ \mathcal{R}_h^i(v_h) &= \mathrm{diag}(\mathrm{S}^{\mathrm{i}-1}, \mathrm{I})(\tilde{\mathcal{R}}_{\mathrm{h}}^{\mathrm{i}} - \mathrm{col}(\mathrm{T}^{\mathrm{i}}, 0)), \\ \mathcal{R}_d^i(v_h) &= \mathrm{diag}(\mathrm{S}^{\mathrm{i}-1}, \mathrm{I})(\tilde{\mathcal{R}}_{\mathrm{d}}^{\mathrm{i}} - \mathrm{col}(\mathrm{T}^{\mathrm{i}}, 0)), \end{aligned}$$

where $\mathrm{col}(\mathrm{T}^{\mathrm{i}}, 0)$ is a column vector built by stacking the zero vector under the vector T^i.

[4]The notation $S^i \mathcal{P}_a + T^i$ with $S^i \in \mathbb{R}^{2\times 2}$, $\mathcal{P}_a \in \mathbb{R}^2$ and $T^i \in \mathbb{R}^2$, denotes the set defined by

$$\{x \in \mathbb{R}^2 | x = S^i y + T^i, y \in \mathcal{P}_a\}.$$

.

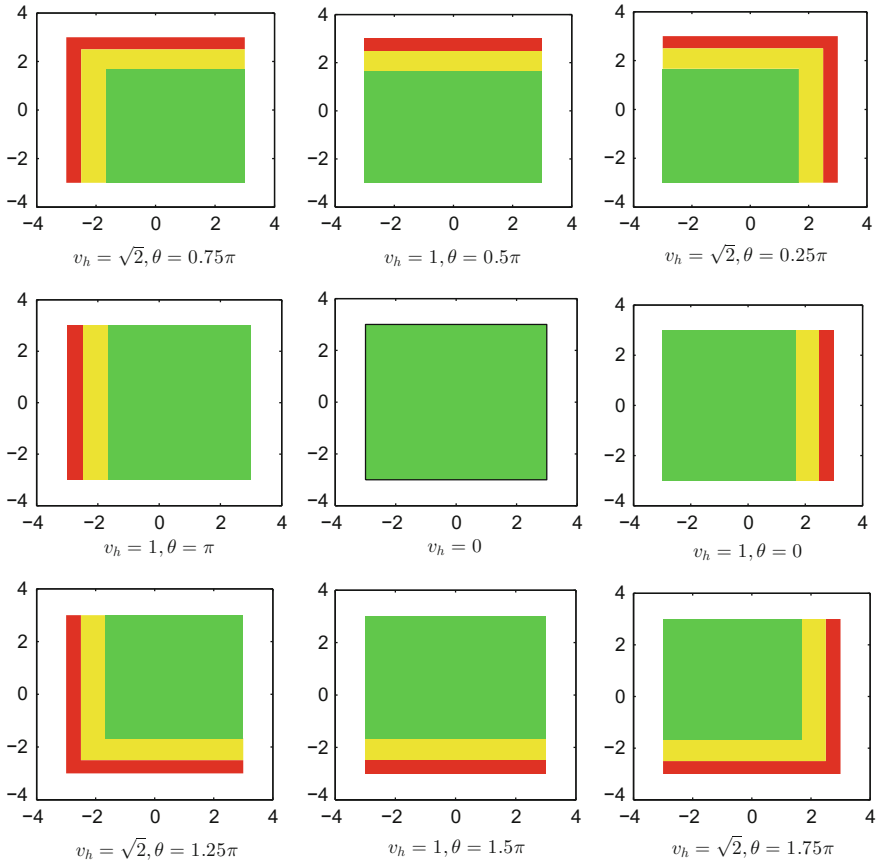

Fig. 2.3 Illustration of the safe (*green*), the hysteresis (*yellow*) and the dangerous subsets (*red*) for the case $n = 2$ ($b_1 = 1, b_2 = 2$)

The sharing function relative to the i^{th} group of constraints can then be defined as

$$k^i(p, \theta, v_h) = \begin{cases} 0, \ (p, \theta, \phi) \in \mathcal{R}_d^i(v_h) \text{ and } L^i = \min\limits_{j=I_1}^{I_{n_c}} L^j, \\ l^i, \ (p, \theta, \phi) \in \mathcal{R}_h^i(v_h), \\ 1, \ \text{otherwise}, \end{cases} \tag{2.13}$$

where

$$l^i = \begin{cases} 1, \text{ if } k^i(t^-) = 0, \\ 0, \text{ if } k^i(t^-) = 1. \end{cases}$$

Note that in the cases in which two constraints are active, there is only one group of active constraints. However, if only one constraint is active, there could be n_c groups of active constraints, where $n_c \leq m - 1$. Therefore, the activation of the i^{th} group of constraints does not imply the activation of the i^{th} feedback controller u_f^i.

Suppose $I_1, I_2, \ldots, I_{n_c}$ groups of constraints are active at the time instant t, where $I_i \in \{1, 2, \ldots, N_c\}$ for all $i \in \{1, 2, \ldots, n_c\}$ and L^j is defined in Eq. (2.9).

Finally, the shared-control input u_s is given as

$$\begin{aligned} u_s(p, \theta, \phi, v_h) = &\sum_{i=1}^{N_c} [(1 - k^i(p, \theta, v_h)) u_f^i(p, \theta, \phi, p_r, \theta_r, \alpha_r)] \\ &+ \min_{i=1}^{N_c} k^i(p, \theta, v_h)\, u_h(t). \end{aligned} \tag{2.14}$$

Proposition 2.1 *Consider the kinematic model of a rear-wheel car (2.1) with the shared-control algorithm (2.10)–(2.13) and (2.14). Let $\mathcal{P}_a$ be a given compact and nonempty admissible Cartesian configuration set described by (2.3) and u_h be a given h-control. Assume $(x(0), y(0)) \in \mathcal{P}_a$. Then there exists positive γ_1, γ_2, γ_3 and $b_2 > b_1 > 0$ such that the following properties hold for the s-closed-loop system.*

i) $(x(t), y(t)) \in \mathcal{P}_a$ *for all* $t \geq 0$.
ii) $\Omega_s = \Pi_{\mathcal{R}_s}(\Omega_h)$.
iii) $u_s(t) = u_h(t)$ *for all* $t \geq 0$ *such that* $(p(t), \theta(t), \phi(t)) \in \mathcal{R}_s(v_h(t))$.

Proof To begin with, as detailed in Sect. 2.3.1, the f-control is such that the Cartesian configuration of the system stays in the admissible set $\mathcal{P}_a$. In addition, as detailed in [7] any trajectory should enter the dangerous subset $\mathcal{R}_d$ before leaving $\mathcal{R}$ where u_f is active. Therefore, the set $\mathcal{R}$ is forward invariant and claim i) holds.

Claim ii) is a consequence of the general results in [18], and of the fact that $\Pi_{\mathcal{R}_s}(\Omega_h)$ is the Ω-limit set of both the h-closed-loop and the f-closed-loop systems (by definition, the former, and by Eqs. (2.5)–(2.9), the latter).

Finally, claim iii) is a direct consequence of the definition of the shared-control input u_s.

2.4 Disturbance Rejections

The model studied in Sect. 2.3 does not include uncertainties. In this section, we include additive disturbances to the system dynamics to make the model more flexible and then provide a solution to the underlying robust shared-control problem.

The dynamics of the kinematic model of a rear-wheel drive car with disturbances can be written as

$$\begin{aligned} \dot{x} &= v_s \cos\theta + d_x, \\ \dot{y} &= v_s \sin\theta + d_y, \\ \dot{\theta} &= \frac{v_s \tan\phi}{l} + d_\theta, \\ \dot{\phi} &= \omega_s + d_\phi, \end{aligned} \tag{2.15}$$

where d_x, d_y, d_θ and d_ϕ are disturbances on the dynamics of x, y, θ and ϕ, respectively.

Assumption 2.3 The disturbances are bounded, *i.e.,* $|d_x| \le d_1$, $|d_y| \le d_2$, $|d_\theta| \le d_3$ and $|d_\phi| \le d_4$, where d_1, d_2, d_3 and d_4 are positive constants known to the users.

We assume that Assumptions 2.2 and 2.3 hold for the rest of this section.

With the use of z^i defined in (2.5), system (2.15) with the feedbacks controller u_f^i can be rewritten as

$$\begin{aligned}
\dot{z}_1^i &= \frac{s_{11}^i(v_f^i\cos\theta + d_x) + s_{12}^i(v_f^i\sin\theta + d_y)}{e^{z_1^i}q_{r_1}^i} - \frac{q_{r_1}^i}{q_{r_1}^i},\\
\dot{z}_2^i &= \frac{s_{21}^i(v_f^i\cos\theta + d_x) + s_{22}^i(v_f^i\sin\theta + d_y)}{e^{z_2^i}q_{r_2}^i} - \frac{q_{r_2}^i}{q_{r_2}^i},\\
\dot{\theta} &= \frac{v_f^i\tan\phi}{l} + d_\theta,\\
\dot{\phi} &= \omega_f^i + d_\phi,
\end{aligned} \tag{2.16}$$

where q_r^i is defined by (2.6) and $S^i = [{s_1^i}^T, {s_2^i}^T]^T$ with $s_1^i = [s_{11}^i, s_{12}^i]$ and $s_2^i = [s_{21}^i, s_{22}^i]$.

Let

$$\tan\phi^{i*} = \frac{l}{v_f^i}\begin{bmatrix}
\dot{\theta}^{i*} - f(\theta-\theta^{i*})d_3 + \dfrac{z_1^i v_f^i s_{11}^i}{m_{r_1}^i e^{z_1^i}}\sin\dfrac{\theta+\theta^{i*}}{2}\operatorname{sinc}\dfrac{\theta+\theta^{i*}}{2}\\
-\dfrac{z_1^i v_f^i s_{12}^i}{m_{r_1}^i e^{z_1^i}}\cos\dfrac{\theta+\theta^{i*}}{2}\operatorname{sinc}\dfrac{\theta+\theta^{i*}}{2}\\
+\dfrac{z_2^i v_f^i s_{21}^i}{m_{r_2}^i e^{z_2^i}}\sin\dfrac{\theta+\theta^{i*}}{2}\operatorname{sinc}\dfrac{\theta+\theta^{i*}}{2}\\
-\dfrac{z_2^i v_f^i s_{22}^i}{m_{r_2}^i e^{z_2^i}}\cos\dfrac{\theta+\theta^{i*}}{2}\operatorname{sinc}\dfrac{\theta+\theta^{i*}}{2}
\end{bmatrix},$$

$$S^i\begin{bmatrix} v_f^i\cos\theta^{i*}\\ v_f^i\sin\theta^{i*}\end{bmatrix} = \begin{bmatrix} s_{11}^i f(s_{11}^i z_1^i)d_1 + s_{12}^i f(s_{12}^i z_1^i)d_2 + e^{z_1^i}(\dot{m}_{r_1}^i + \gamma_1 z_1^i)\\ s_{21}^i f(s_{21}^i z_2^i)d_1 + s_{22}^i f(s_{12}^i z_2^i)d_2 + e^{z_2^i}(\dot{m}_{r_2}^i + \gamma_2 z_2^i)\end{bmatrix} = \begin{bmatrix}\beta\\ \zeta\end{bmatrix}, \tag{2.17}$$

where γ_1 and γ_2 are two user-selected positive constants. As stated in Sect. 2.3.1, S^i is invertible. Define $m^i = [m_1^i, m_2^i]^T$ as

$$\begin{bmatrix} m_1^i\\ m_2^i\end{bmatrix} = \begin{bmatrix} v_f^i\cos\theta^{i*}\\ v_f^i\sin\theta^{i*}\end{bmatrix} = {S^i}^{-1}\begin{bmatrix}\beta\\ \zeta\end{bmatrix}.$$

Then v_f^i and θ^{i*} can be calculated as[5]

[5] Recall that the definition of the function atg$(\cdot)$ is given in [8].

$$v_f^i = \sqrt{(m_1^i)^2 + (m_2^i)^2}, \quad \theta^{i*} = \text{atg}(m_2^i, m_1^i). \tag{2.18}$$

Consider the Lyapunov function (2.9) with θ^{i*} and $\tan\phi^{i*}$ defined by (2.18) and (2.17), respectively. Select ω_f^i, together with v_f^i given by (2.18), such that the derivative of L^i satisfies

$$\dot{L}^i \leq -k_1(z_1^i)^2 - k_2(z_2^i)^2 - k_3(\tan\phi - \tan\phi^{i*})^2 + K,$$

where $k_i > 0$ for all $i \in \{1, 2, 3\}$, and K is a positive constant. One such selection is given by

$$\begin{aligned}\omega_f^i = \cos^2\phi \left[\frac{\dot{\phi}^{i*}}{\cos^2\phi^{i*}} - \gamma_3(\tan\phi - \tan\phi^{i*}) - \frac{v_f^i}{l}(\theta - \theta^{i*}) \right] \\ - d_4\epsilon \tanh\frac{c(\tan\phi - \tan\phi^{i*})}{\epsilon},\end{aligned} \tag{2.19}$$

yielding

$$\dot{L}^i \leq \frac{\gamma_1(z_1^i)^2}{q_{r_1}^i} + \frac{\gamma_2(z_2^i)^2}{q_{r_2}^i} - \gamma_3(\tan\phi - \tan\phi^{i*})^2 + K, \tag{2.20}$$

where

$$\begin{aligned}K = \frac{-(\epsilon+1)}{2c(\epsilon-1)} \ln\frac{\epsilon+1}{\epsilon-1} \left(d_1 e^{\frac{\epsilon}{2c|s_{11}^i|}} + d_2 e^{\frac{\epsilon}{2c|s_{12}^i|}} \right) + \frac{\epsilon}{2c} d_3 \ln\frac{\epsilon+1}{\epsilon-1} \\ - \frac{(\epsilon+1)}{2c(\epsilon-1)} \ln\frac{\epsilon+1}{\epsilon-1} \left(d_1 e^{\frac{\epsilon}{2c|s_{21}^i|}} + d_2 e^{\frac{\epsilon}{2c|s_{22}^i|}} \right).\end{aligned}$$

with $c > 0$ and $\epsilon > 1$ user-selected constants.

Note that by choosing proper values of ϵ and c, we can render K arbitrarily small. In addition, (2.20) indicates that

$$\lim_{t\to\infty} |z_1^i| \leq \sqrt{-Kq_{r_1}^i/\gamma_1}, \quad \lim_{t\to\infty} |z_2^i| \leq \sqrt{-Kq_{r_2}^i/\gamma_2}.$$

This discussion is summarized in the following statement.

Proposition 2.2 *Consider the system (2.15) with the feedback controller* $u_f^i = [v_f^i, \omega_f^i]^T$ *given by (2.18) and (2.19). In addition,* q_r^i, θ^{i*} *and* $\tan\phi^{i*}$ *are given by (2.6), (2.18) and (2.17), respectively. Assume that the admissible configuration set of the car* $\mathcal{P}_a$ *is defined by (2.3) and* $(x(0), y(0)) \in \mathcal{P}_a$. *Then the closed-loop system has the following properties.*

i) $(x(t), y(t)) \in \mathcal{P}_a$ *for all* $t \geq 0$.
ii) Define the tracking errors as $e^i(t) = [e^i_x(t), e^i_y(t)]^T$ *with*

$$e^i_x(t) = \left| |\frac{x(t)}{x^i_r(t)}| - 1 \right|, \quad e^i_y(t) = \left| |\frac{y(t)}{y^i_r(t)}| - 1 \right|.$$

Then $\lim_{t\to\infty} e^i(t)$ *is bounded and the bound can be controlled by tuning the parameters,* $\gamma_1, \gamma_2, \epsilon$ *and* c*, of the feedback controller.*

Remark 2.1 According to (2.17) $\tan\phi^{i*}$ is not defined when $v^i_f = 0$. In this case, we redesign the feedback controller as

$$\omega^i_f = \omega^i_r - \text{sign}(\phi - \phi^i_r)d_4 - \gamma_4(\phi - \phi^i_r), \tag{2.21}$$

with $\gamma_4 > 0$.

Consider the Lyapunov function[6] $L^i = \frac{1}{2}(\phi - \phi^i_r)^2$ with ω^i_f given by (2.21), then the derivative of L^i is calculated as

$$\begin{aligned}\dot{L}^i &= (\phi - \phi^i_r)(\omega^i_f + d_\phi - \omega^i_r) = (\phi - \phi^i_r)[d_\phi - \text{sign}(\phi - \phi^i_r)d_4 - \gamma_4(\phi - \phi^i_r)] \\ &\leq -\gamma_4(\phi - \phi^i_r)^2 \leq 0.\end{aligned}$$

2.5 Design of the Shared Control Without Measurements of Absolute Positions

In this section, we discuss how to design the shared controller for the kinematic model of a rear-wheel drive car without absolute positioning while satisfying all the properties given in Sect. 2.2 for any nonempty admissible configuration set. In the rest of this section, we assume that the measurements are the distance to the obstacle along the current forward direction D, the angular difference between the real and the reference heading angle θ_e, the wheel angle ϕ and the distances to the obstacles along and orthogonal to the reference forward direction, d_1 and

$$d_2 = \begin{cases} d_{2l}, & \text{if } |\log\dfrac{d_{2l} - \tilde{d}_2}{d_{r_{2l}} - \tilde{d}_2}| \leq |\log\dfrac{d_{2r} - \tilde{d}_2}{d_{r_{2r}} - \tilde{d}_2}|, \\ d_{2r}, & \text{if } |\log\dfrac{d_{2l} - \tilde{d}_2}{d_{r_{2l}} - \tilde{d}_2}| > |\log\dfrac{d_{2r} - \tilde{d}_2}{d_{r_{2r}} - \tilde{d}_2}|, \end{cases}$$

where d_{2l} and d_{2r} denote the distances to the obstacles on the left-hand side and right-hand side orthogonal to the reference forward direction, respectively. In addition, $\tilde{d}_2$ is given in Sect. 2.5.1.

[6]Note that this is a Lyapunov function only for the ϕ system.

2.5.1 Design of the Feedback Controller

According to the definition of d_2, $d_2 = d_{2l}$ or $d_2 = d_{2r}$. Without loss of generality, we provide the design of the shared controller only for the case in which $d_2 = d_{2l}$. The dynamics of the closed-loop system with the feedback controller $u_f = [v_f, \omega_f]^T$ can be written, using the variables d_1, d_2, θ_e and ϕ, as

$$\begin{aligned} \dot{d}_1 &= -v_f \cos\theta_e, \\ \dot{d}_2 &= -v_f \sin\theta_e, \\ \dot{\theta}_e &= \frac{v_f \tan\phi - v_r \tan\phi_r}{l}, \\ \dot{\phi} &= \omega_f. \end{aligned} \tag{2.22}$$

In addition, for any nonempty admissible configuration set $\mathcal{P}_a$, the constraint $(x(t), y(t)) \in \mathcal{P}_a$ can be rewritten as

$$d_i(t) \geq \tilde{d}_i, \quad \forall i \in \{1, 2\}, \tag{2.23}$$

where $\tilde{d}_i$ is a positive constant. One choice for $\tilde{d}_1$ and $\tilde{d}_2$ is $\tilde{d}_1 = \tilde{d}_2 = \sqrt{l^2 + (\frac{w}{2})^2}$.

Assumption 2.4 The signals d_{d_1} and d_{d_2}, describing the desired distances to the relative obstacles (the obstacles along and orthogonal to the reference forward direction), are continuous.

The previous assumption holds for the rest of this section.

Define the variable $z = [z_1, z_2]^T$, based on the measurements of distances, as

$$z_i = \log \frac{d_i - \tilde{d}_i}{d_{r_i} - \tilde{d}_i}, \forall i \in \{1, 2\}, \tag{2.24}$$

where d_{r_1} and d_{r_2} are the feasible reference signal relative to d_1 and d_2, respectively and are defined as

$$d_{r_i} = \begin{cases} d_{d_i}, & \text{if } d_{d_i} \geq (1 - \frac{\sqrt{2}}{2})r + \epsilon + \tilde{d}_i, \\ \epsilon + \tilde{d}_i, & \text{if } d_{d_i} \leq (1 - \sqrt{2})r + \epsilon + \tilde{d}_i, \\ m_i, & \text{otherwise}, \end{cases} \tag{2.25}$$

where $m_i = r + \epsilon + \tilde{d}_i - \sqrt{r^2 - [(\sqrt{2} - 1)r - \epsilon + d_{d_i} - \tilde{d}_i]^2}$ and ϵ is a sufficiently small positive constant. Note that d_{r_i} is a smooth continuous function, indicating that $\dot{d}_{r_i}$ exists.

Suppose $(d_{d_1}, d_{d_2}, \theta_d, \phi_d)$ belongs to the Ω-limit set for the h-closed-loop system, *i.e.,* $(d_{d_1}, d_{d_2}, \theta_d, \phi_d) \in \Omega_h$, then the projection of it into the safe subset $\mathcal{R}_s$ is given by

$$\Pi_{\mathcal{R}_s}(d_{d_1}, d_{d_2}, \theta_d, \phi_d) = (d_{r_1}, d_{r_2}, \theta_d, \phi_d),$$

where d_{r_1} and d_{r_2} are defined by (2.25). Hence, the projection of Ω_h into the safe subset $\mathcal{R}_s$ is defined as

$$\Pi_{\mathcal{R}_s}(\Omega_h) = \left\{ s \in \mathcal{R}_s \,\middle|\, s = \Pi_{\mathcal{R}_s}(d_{d_1}, d_{d_2}, \theta_d, \phi_d), \quad \forall (d_{d_1}, d_{d_2}, \theta_d, \phi_d) \in \Omega_h \right\}.$$

With the variable z given by (2.24), system (2.22) can be written as

$$\begin{aligned}
\dot{z}_1 &= \frac{v_r}{d_{r_1} - \tilde{d}_1} - \frac{v_f \cos\theta_e}{d_1 - \tilde{d}_1}, \\
\dot{z}_2 &= -\frac{v_f \sin\theta_e}{d_2 - \tilde{d}_2}, \\
\dot{\theta}_e &= \frac{v_f \tan\phi - v_r \tan\phi_r}{l}, \\
\dot{\phi} &= \omega_f.
\end{aligned}$$

Let[7]

$$\theta_e^* = \mathrm{atg}\left(\gamma_2(d_2 - \tilde{d}_2)z_2, (d_1 - \tilde{d}_1)\left(\frac{v_r}{d_{r_1} - \tilde{d}_1} + \gamma_1 z_1\right)\right), \tag{2.26a}$$

$$\xi = \sqrt{(\gamma_2(d_2 - \tilde{d}_2)z_2)^2 + \left[(d_1 - \tilde{d}_1)\left(\frac{v_r}{d_{r_1} - \tilde{d}_1} + \gamma_1 z_1\right)\right]^2}, \tag{2.26b}$$

$$\phi^* = \mathrm{atg}\left(\begin{array}{c} \dfrac{lz_2}{d_2 - \tilde{d}_2}\cos\dfrac{\theta_e + \theta_e^*}{2}\mathrm{sinc}\dfrac{\theta_e - \theta_e^*}{2} + \dfrac{v_r \tan\phi_r}{\xi} \\ -\dfrac{lz_1}{d_1 - \tilde{d}_1}\sin\dfrac{\theta_e + \theta_e^*}{2}\mathrm{sinc}\dfrac{\theta_e - \theta_e^*}{2} + \dfrac{l\dot{\theta}_e^*}{\xi} \end{array}, 1\right), \tag{2.26c}$$

where $\gamma_1 > 0$, $\gamma_2 > 0$.

Consider the Lyapunov function

$$L(z_1, z_2, \theta_e, \phi, t) = \frac{1}{2}[z_1^2 + z_2^2 + (\theta_e - \theta_e^*)^2 + (\tan\phi - \tan\phi^*)^2], \tag{2.27}$$

and choose v_f and ω_f such that $\dot{L}(t) < 0$ for all $t \geq 0$ and $(z_1, z_2, \theta_e, \tan\phi) \neq (0, 0, 0, \tan\phi_r)$. One such a choice is given by

$$\begin{aligned}
v_f &= \xi, \\
\omega_f &= \cos^2\phi\left[\frac{\dot{\phi}^*}{\cos^2\phi^*} - \frac{v(\theta_e - \theta_e^*)}{l} - \gamma_3(\tan\phi - \tan\phi^*)\right],
\end{aligned}$$

[7] Recall that the definition of the function atg(·) is given in [8].

where γ_3 is a positive constant. This can be transfered into the $(d_1, d_2, \theta_e, \phi)$ coordinates by

$$v_f = \sqrt{(d_1 - \tilde{d}_1)^2 \left(\frac{v_r}{d_{r_1} - \tilde{d}_1} + \gamma_1 \log \frac{d_1 - \tilde{d}_1}{d_{r_1} - \tilde{d}_1} \right)^2 + \gamma_2^2 (d_2 - \tilde{d}_2)^2 \log^2 \frac{d_2 - \tilde{d}_2}{d_{r_2} - \tilde{d}_2}},$$
$$\omega_f = \cos^2 \phi \left[\frac{\dot{\phi}^*}{\cos^2 \phi^*} - \frac{v(\theta_e - \theta_e^*)}{l} - \gamma_3 (\tan \phi - \tan \phi^*) \right], \tag{2.28}$$

where

$$\theta_e^* = \text{atg} \left(\gamma_2 (d_2 - \tilde{d}_2) \log \frac{d_2 - \tilde{d}_2}{d_{r_2} - \tilde{d}_2}, (d_1 - \tilde{d}_1) \left(\frac{v_r}{d_{r_1} - \tilde{d}_1} + \gamma_1 \log \frac{d_1 - \tilde{d}_1}{d_{r_1} - \tilde{d}_1} \right) \right),$$
$$\phi^* = \text{atg} \left(\begin{array}{c} \dfrac{l}{d_2 - \tilde{d}_2} \log \dfrac{d_2 - \tilde{d}_2}{d_{r_2} - \tilde{d}_2} \cos \dfrac{\theta_e + \theta_e^*}{2} \text{sinc} \dfrac{\theta_e - \theta_e^*}{2} + \dfrac{v_r \tan \phi_r}{v_f} \\ - \dfrac{l}{d_1 - \tilde{d}_1} \log \dfrac{d_1 - \tilde{d}_1}{d_{r_1} - \tilde{d}_1} \sin \dfrac{\theta_e + \theta_e^*}{2} \text{sinc} \dfrac{\theta_e - \theta_e^*}{2} + \dfrac{l \dot{\theta}_e^*}{v_f} \end{array} , 1 \right), \tag{2.29}$$

and $d_r = [d_{r_1}, d_{r_2}]^T$ is given by (2.25).

2.5.2 Shared-Control Algorithm

For any given v_h, the safe, hysteresis, and dangerous subsets can be defined by (30) at the bottom of this page, where D is the measured distance to the obstacles along the current forward direction, b_1 and b_2 are user-selected parameters and $b_2 > b_1 > 0$.

$$\mathcal{R}_s(v_h) = \left\{ (d_1, d_2, \theta_e, \phi) \in \mathbb{R}^+ \times \mathbb{R}^+ \times \mathbb{S} \times \mathbb{S} : v_h < \frac{1}{b_2 - D} - \frac{1}{b_2} \text{ if } D \leq b_2 \right\}$$

$$\mathcal{R}_h(v_h) = \left\{ \begin{array}{l} (d_1, d_2, \theta_e, \phi) \in \mathbb{R}^+ \times \mathbb{R}^+ \times \mathbb{S} \times \mathbb{S} : v_h \leq \dfrac{1}{b_1 - D} - \dfrac{1}{b_1} \\ \qquad \text{and } v_h \geq \dfrac{1}{b_2 - D} - \dfrac{1}{b_2} \\ \qquad \text{and } D \leq b_1 \\ \qquad \text{or } \ v_h \geq \dfrac{1}{b_2 - D} - \dfrac{1}{b_2} \\ \qquad \text{and } b_1 \leq D \leq b_2 \end{array} \right\}$$

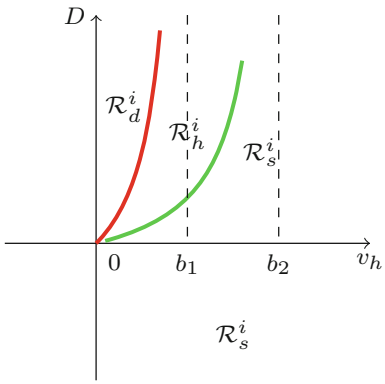

Fig. 2.4 Illustration of the safe, the hysteresis and the dangerous sets with measurements of D and v_h

$$\mathcal{R}_d(v_h) = \left\{ (d_1, d_2, \theta_e, \phi) \in \mathbb{R}^+ \times \mathbb{R}^+ \times \mathbb{S} \times \mathbb{S} : v_h > \frac{1}{b_1 - D} - \frac{1}{b_1} \text{ and } 0 \le D \le b_1 \right\} \tag{2.30}$$

Figure 2.4 illustrates how the overall set is divided into three subsets based on v_h and D. Basically, the state belongs to the dangerous set if D is close to zero (*i.e.,* $0 \le D \le b_1$) and v_h is large (*i.e.,* (D, v_h) is located above the red curve); the state belongs to the safe subset if D is large (*i.e.,* $D > b_2$) or v_h is small (*i.e.,* (D, v_h) is located below the green curve).

The sharing function k can then be defined as

$$k(D, v_h) = \begin{cases} 1, & (d_1, d_2, \theta_e, \phi) \in \mathcal{R}_s(v_h), \\ l, & (d_1, d_2, \theta_e, \phi) \in \mathcal{R}_h(v_h), \\ 0, & (d_1, d_2, \theta_e, \phi) \in \mathcal{R}_d(v_h), \end{cases} \tag{2.31}$$

where

$$l = \begin{cases} 1, \text{ if } (d_1, d_2, \theta_e, \phi) \text{ enters } \mathcal{R}_h(v_h) \text{ from } \mathcal{R}_s(v_h), \\ 0, \text{ if } (d_1, d_2, \theta_e, \phi) \text{ enters } \mathcal{R}_h(v_h) \text{ from } \mathcal{R}_d(v_h). \end{cases}$$

Finally, the shared-control input of the system (2.22) is given as

$$u_s = (1 - k(D, v_h))u_f(d, d_r, \theta_e, \phi, v_r) + k(D, v_h)u_h. \tag{2.32}$$

The following statement summarizes the discussions in this section without proof.

Proposition 2.3 *Consider the kinematic model of a rear-wheel drive car controlled by the shared-control law (2.28)–(2.31) and (2.32) without absolute positioning, the dynamics of which can be described by (2.22). Assume that the admissible Cartesian configuration set of the car is nonempty and the initial position of the car is feasible,*

i.e., $(x(0), y(0)) \in \mathcal{P}_a, d_1(0) > \tilde{d}_1, d_2(0) > \tilde{d}_2$. *Let* u_h *be a given h-control. Then there exists positive* $\gamma_1, \gamma_2, \gamma_3$, *and* $b_2 > b_1 > 0$ *such that the closed-loop system has the following properties.*

i) $d_1(t) > \tilde{d}_1$ *and* $d_2(t) > \tilde{d}_2$ *for all* $t \geq 0$;
ii) $\Omega_s = \Pi_{\mathcal{R}_s}(\Omega_h)$;
iii) $u_s(t) = u_h(t)$ *for all* t *such that* $(d_1(t), d_2(t), \theta_e(t), \phi(t)) \in \mathcal{R}_s$.

Remark 2.2 In the cases in which $\tilde{d}_1 = \tilde{d}_2 = \sqrt{l^2 + (\frac{w}{2})^2}$, the car is unable to reach the boundary of its admissible configuration set (such as parking next to the curb). However, this can be easily solved by modifying the values of $\tilde{d}_1$ and $\tilde{sd}_2$ to l and $\frac{w}{2}$, respectively when θ_e is close to zero.

Remark 2.3 According to the shared-control input (2.28)–(2.31) and (2.32), the feedback controller is active only if the position of the car is "close" to the boundary of $\mathcal{P}_a$. Therefore, d_i can be changed to $\hat{d}_i = \min(d_i, \mathcal{B})$ for both $i \in \{1, 2\}$, where $\mathcal{B}$ is a positive user-selected constant.

As a result one can design the feedback controller only for the cases in which $d_i \leq \mathcal{B}$. This is helpful in real applications, especially when the obstacle is exactly in parallel or orthogonal to the required direction, *i.e.,* $d_1 = \infty$ or $d_2 = \infty$.

2.6 Case Studies

This section provides three case studies to illustrate how the shared-control algorithm works and demonstrates that it is effective in guaranteeing the safety of the car in various situations. The first case study deals with the situation in which absolute positions are not available, while the other two show how the vehicle controlled by the shared controller behaves in the presence of disturbances.

2.6.1 Case I: Turning Without Absolute Positioning

Consider the kinematic model of a rear-wheel drive car described by the Eq. (2.22) and controlled by the shared-control law (2.28)–(2.31) and (2.32). Assume that the absolute positions are not measurable and that the controlled car is approaching a junction with busy traffic on the main road. The driver wants to turn left and continue his/her journey on the main road but does not check the traffic carefully. Therefore, he/she makes the wrong decision at the junction and puts himself/herself in a dangerous situation.

Simulation results are given in Fig. 2.5, where the controlled car changes its color from green to red indicating that the feedback controller is active and gains the control authority from the driver to keep him/her safe. With the help of the shared controller,

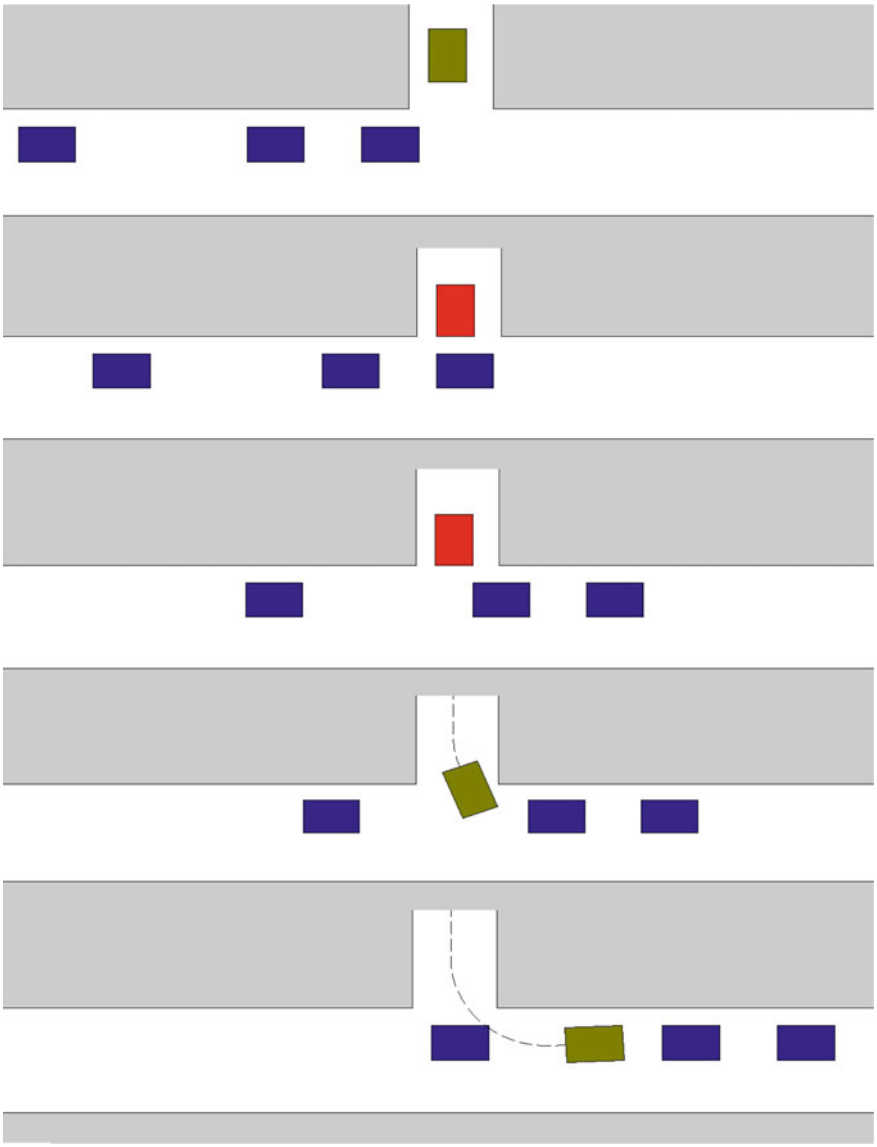

Fig. 2.5 Snapshots of the path of the car with the shared control in the (x, y)-plane for the set $\mathcal{P}_a$ represented by the *white* area. *Green* car: the controlled car (the feedback controller is not active). *Red* car: the controlled car (the feedback controller is active). *Blue* cars: the other vehicles on the road. Dashed line: (x, y)-trajectory of the controlled car

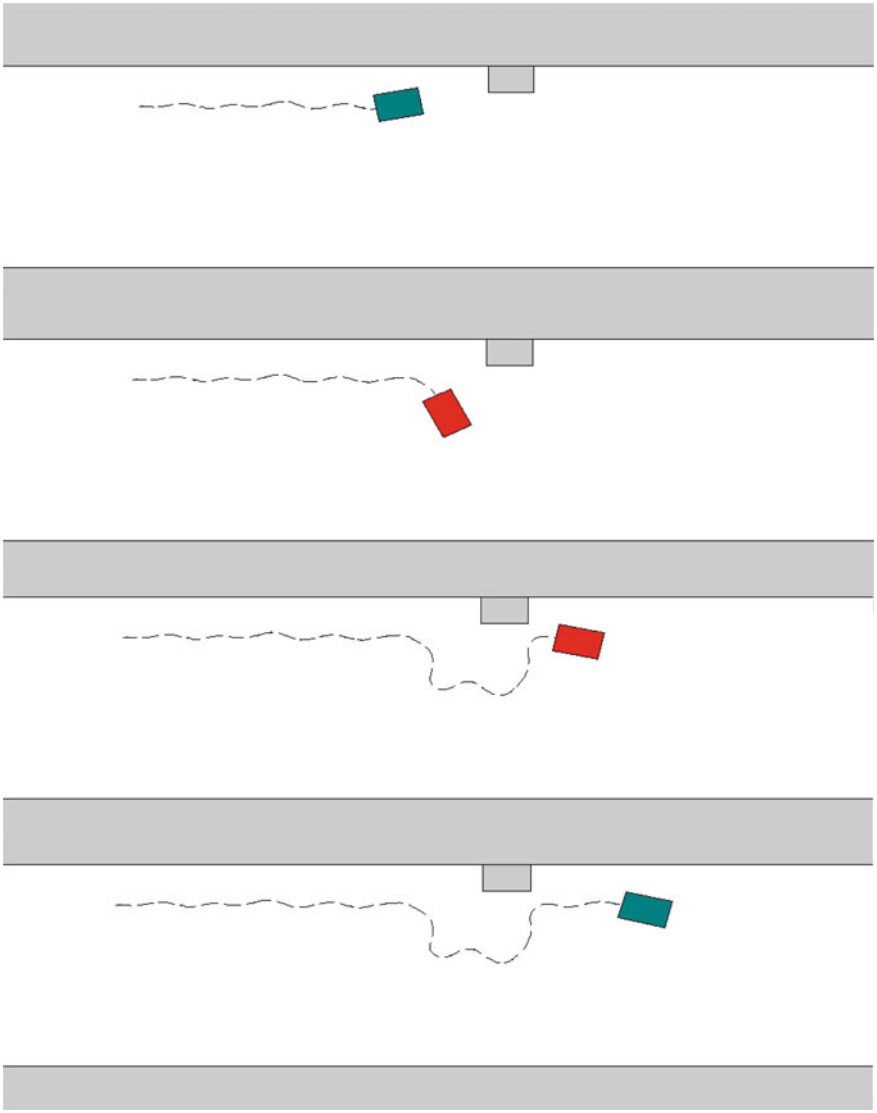

Fig. 2.6 Snapshots of the path of the car with the shared control in the (x, y)-plane for the set $\mathcal{P}_a$ represented by the *white* area. *Green* car: the controlled car (the feedback controller is not active). *Red* car: the controlled car (the feedback controller is active). *Grey* car: the parked car. Dashed line: (x, y)-trajectory of the controlled car

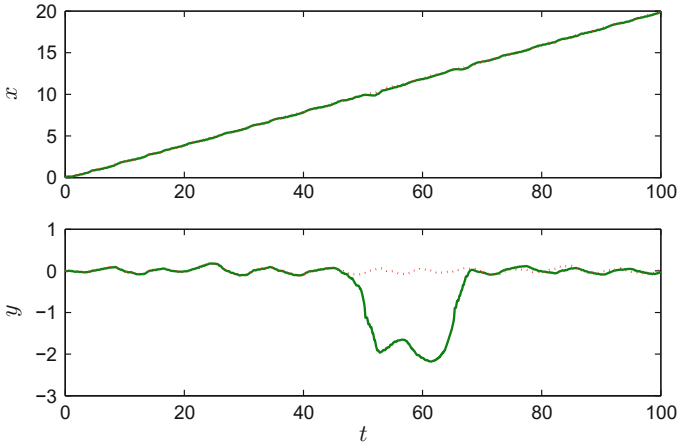

Fig. 2.7 Time histories of the variables x and y for the h-closed-loop system (*red*, dotted) and for the s-closed-loop system (*green*, solid)

the car stops at the junction and waits until there is a sufficiently long gap to make the turn. Finally, the car leaves the junction and turns left joining the main road safely.

2.6.2 Case II: Driving on a Road with Parked Cars

This case studies the shared control of a rear-wheel drive car with disturbances. We assume that all disturbances are random numbers between -0.1 and 0.1. The controlled car is driven on a road with parked cars. Simulation results are displayed in Figs. 2.6 and 2.7. Figure 2.6 shows that the car stays in the feasible configuration set $\mathcal{P}_a$ represented by the white areas, demonstrating the effectiveness of the shared controller. Figure 2.7 shows that the (x, y)-trajectory of the car is not smooth and is full of oscillations. This is because of the unknown disturbances. However, even though the model is not perfect and the driver does not recognize the parked car on his/her lane, the controlled car is able to bypass it and continue its journey. Furthermore, the distance from the controlled car to the parked car is more than we expect because we add additional space to compensate the bounded tracking error when designing the feedback controller.

2.6.3 Case III: Emergency Breaking

Similar to Case II, we assume that the model is imperfect and $d_1 = d_2 = d_3 = d_4 = 0.1$. We also assume that the controlled car is driven on the road, while the car in front of it (represented by the blue rectangle in Fig. 2.8) brakes suddenly. However, the

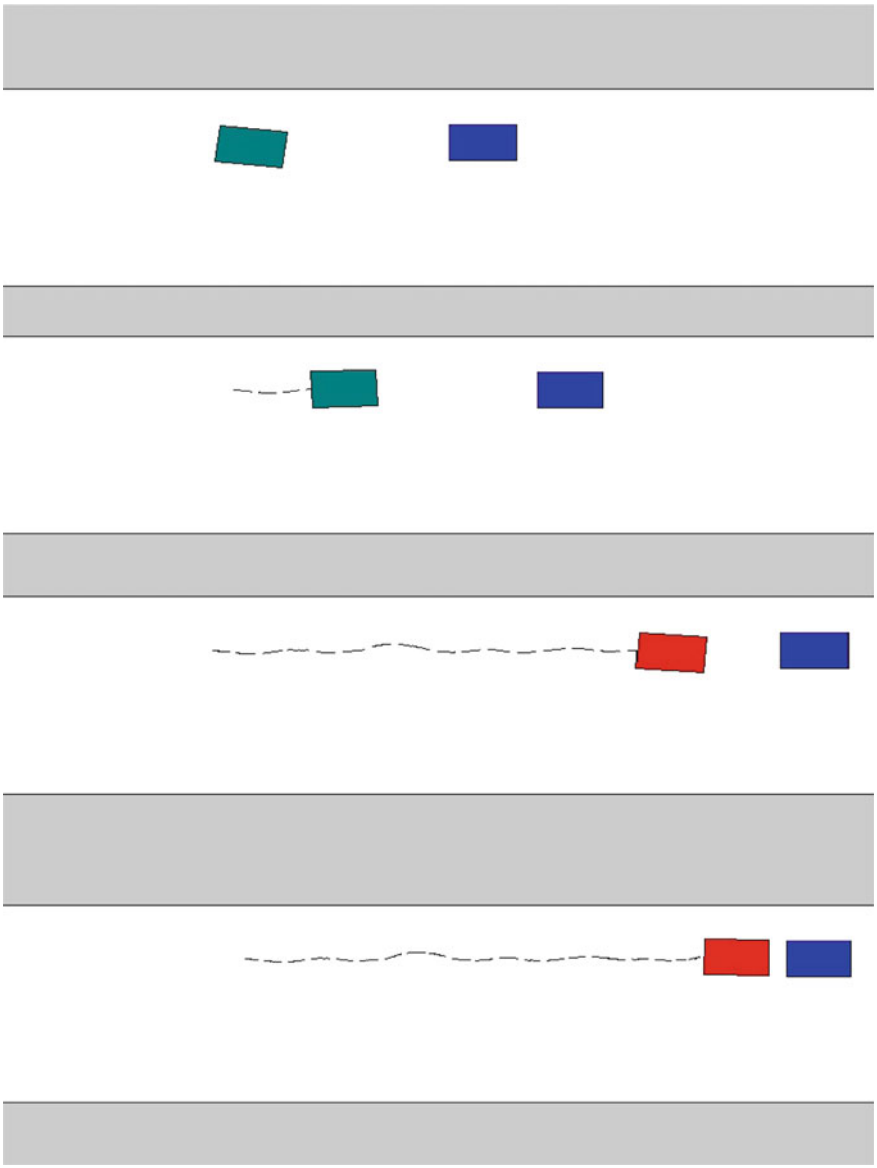

Fig. 2.8 Snapshots of the path of the car with the shared control in the (x, y)-plane for the set $\mathcal{P}_a$ represented by the *white* area. *Green* car: the controlled car (the feedback controller is not active). *Red* car: the controlled car (the feedback controller is active). *Blue* cars: other vehicles on the road. Dashed line: (x, y)-trajectory of the controlled car

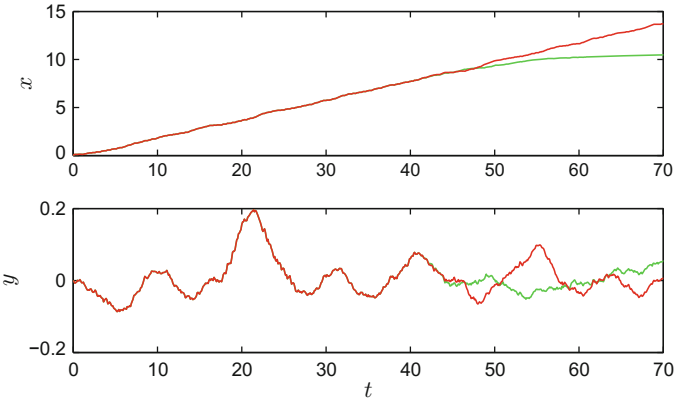

Fig. 2.9 Time histories of the variables x and y for the h-closed-loop system (*red*, dotted) and for the s-closed-loop system (*green*, solid)

driver sitting in the controlled car does not respond to it in time. Simulation results are displayed in Figs. 2.8 and 2.9. Figure 2.8 shows that the car with the shared controller stops behind the blue car at a certain distance to avoid collision even though the driver keeps pressing the gas pedal, hence, demonstrating the effectiveness of the shared-control law. Figure 2.9 indicates that the (x, y)-trajectories of the car for the h-closed-loop system and the s-closed-loop system are the same when $t < 44$ as the controlled car is far away from the car in front.

2.7 Conclusions

This chapter studies the shared-control problem for the kinematic model of a rear-wheel drive car with and without absolute positioning. We present solutions to the problem with static and dynamic admissible configuration sets. In addition, we study the system in the presence of bounded disturbances and prove that the tracking error is bounded. The sharing function, describing how the control authority is shared between the driver and the feedback controller, is defined as a hysteresis switch to reduce oscillations. Three examples are used to demonstrate the effectiveness of the shared-control algorithm. In the future, we will focus on the study of the cooperations between cars and of systems with measurement errors.

References

1. Chiang HH, Wu SJ, Perng JW, Wu BF, Lee TT (2010) The human-in-the-loop design approach to the longitudinal automation system for an intelligent vehicle. IEEE Trans Syst Man Cybern 40(4):708–720

2. Drage T, Kalinowski J, Braunl T (2014) Integration of drive-by-wire with navigation control for a driverless electric race car. IEEE Intell Transp Syst Mag 6(4):23–33
3. Fadilah SI, Shariff ARM (2014) A time gap interval for safe following distance (TGFD) in avoiding car collision in wireless vehicular networks (VANET) environment. In: Proceedings of international conference on intelligent systems, modelling and simulation, pp 683–689
4. Ferrara A, Librino R, Massola A, Miglietta M, Vecchio C (2008) Sliding mode control for urban vehicles platooning. In: Proceedings of IEEE intelligent vehicles symposium, pp 877–882
5. Gnatzig S, Schuller F, Lienkamp M (2012) Human-machine interaction as key technology for driverless driving - a trajectory-based shared autonomy control approach. In: Proceedings of IEEE conference on RO-MAN, Paris, pp 913–918
6. Jiang J, Astolfi A (2013) Shared-control for fully actuated linear mechanical systems. In: Proceedings of IEEE conference on decision and control, Italy
7. Jiang J, Astolfi A (2014) Shared-control for the kinematic model of a mobile robot. In: Proceedings of IEEE conference on decision and control, USA
8. Jiang J, Astolfi A (2015) Shared-control for the kinematic model of a rear-wheel drive car. In: Proceedings of american control conference, USA
9. Jiang J, Astolfi A (2016) Shared-control for typical driving scenarios. In: submitted to european control conference, Denmark
10. Kianfar R, Augusto B, Ebadighajari A, Hakeem U, Nilsson J, Raza A, Tabar RS, Irukulapati NV, Englund C, Falcone P, Papanastasiou S, Svensson L, Wymeersch H (2012) Design and experimental validation of a cooperative driving system in the grand cooperative driving challenge. IEEE Trans Intell Transp Syst 13(3):994–1007
11. Kim JS, Ryu JH (2013) Shared teleoperation of a vehicle with a virtual driving interface. In: Proceedings of IEEE international conference on control, automation and systems, Gwangju, pp 51–857
12. Lee U, Yoon S, Shim HC, Vasseur P (2014) Local path planning in a complex environment for self-driving car. In: Proceedings of IEEE annual international conference on cyber technology in automation, control, and intelligent systems, Hong Kong, pp 445–450
13. Lilly JH (2007) Evolution of a negative-rule fuzzy obstacle avoidance controller for an autonomous vehicle. IEEE Trans Fuzzy Syst 15(4):718–728
14. Massera Filho C, Wolf DF, Grassi V, Osorio FS (2014) Longitudinal and lateral control for autonomous ground vehicles. In: Proceedings of IEEE symposium on intelligent vehicles, pp 588–593
15. McGann C, Py F, Rajan K, Ryan J, Henthorn R (2008) Adaptive control for autonomous underwater vehicles. In: Proceedings of AAAI conference on artificial intelligence, pp 1319–1324
16. Michalek M, Kielczewski M (2013) Helping a driver in backward docking with n-trailer vehicles by the passive control-assistance system. In: Proceedings of IEEE international conference on intelligent transportation systems, pp 1993–1999
17. Mohajerpoor R, Dezfuli SS, Bahadori B (2013) Teleoperation of an unmanned car via robust adaptive backstepping control approach. In: Proceedings of IEEE/ASME international conference on advanced intelligent mechatronics, pp 1540–1545
18. Prieur C (2001) Uniting local and global controllers with robustness to vanishing noise. Math Control Signals Syst 14:143–172
19. Thrun S (2010) Toward robotic cars. Commun ACM 53(4):99–106

20. Wang J, Zhang L, Zhang D, Li K (2009) Cooperative (rather than autonomous) vehicle-highway automation systems. IEEE Intell Transp Syst Mag 1(1):10–19
21. Wang J, Zhang L, Zhang D, Li K (2012) An adaptive longitudinal driving assistance system based on driver characteristics. IEEE Trans Intell Transp Syst 14(1):1–12
22. Zhou SH, Yasunobu S (2006) A cooperative auto-driving system based on fuzzy instruction. In: Proceedings of 7th international symposium on advanced intelligent systems, pp 300–304

http://www.springer.com/978-3-319-40532-2

Trends in Control and Decision-Making for Human–Robot Collaboration Systems

Wang, Y.; Zhang, F. (Eds.)

2017, XIX, 418 p. 173 illus., 121 illus. in color.,
Hardcover
ISBN: 978-3-319-40532-2